Two-channel pitch/yaw missile autopilot design using arbitrary order sliding modes based pole placement

B. Kada
bkada@kau.edu.sa
King Abdulaziz University
Department of Aeronautical Engineering
Jeddah
Saudi Arabia

ABSTRACT

The paper presents a new missile autopilot system design. The design is achieved through the pole-placement in quasi-continuous high-order sliding mode gains adjustment. Enhanced performance, strong robustness and smooth control are obtained through arbitrary increase of the number of non-oscillatory stable poles. The target application of this technique the two-channel pitch/yaw missile autopilot system is considered. Numerical simulations indicate that the arbitrary-order sliding modes based pole placement's performance compares favourably against recently proposed high-order pole placement schemes.

The proposed arbitrary-order pole placement scheme presents a promising design tool for finite-time stabilisation and control of uncertain multivariable systems.

Paper No. 4247. Manuscript received 6 August 2014, revised version received 10 February 2015, accepted 11 February 2015.

https://doi.org/10.1017/S0001924000010812 Published online by Cambridge University Press

1.0 INTRODUCTION

Pole-placement is one of the most popular control tools that have been widely used to design controllers for dynamical systems ranging from linear to nonlinear systems. If a linear system is completely controllable and observable, a strict pole-placement is achievable in a transfer function or state space context using a classical eigenvalue assignment. Within state-feedback control framework, pole-placement provides a convenient strategy to achieve desired closed-loop transient response, stability and convergence rate. Various constructive pole assignment algorithms for linear dynamic systems have been reported in the literature[1-9]. However, many of these algorithms are computationally unstable, sensitive to parameter uncertainties and disturbances and unable to deal with non-convex constraints.

For nonlinear uncertain systems, robust pole-placement is necessary to ensure parameter uncertainties compensation and disturbances cancellation. Based upon the local controllability characteristic of nonlinear systems, non-strict or partial pole-placement can be obtained and local robust performance can be achieved around desired trim conditions or desirable locations. Different robust pole-placement schemes have been developed in the last few years. See for example[10-23], for both continuous and discrete systems.

Since the publication of Ackermann-Utkin's formula as sliding mode-based pole-placement scheme[24], many studies have investigated the application of sliding mode approach in the design of robust pole-placement controllers[25-30]. Sliding mode-based pole-placement guarantees robustness against matched and unmatched disturbances while driven the sliding variables to their zero-level. Nevertheless, the standard sliding modes are bounded by some restrictions; their implementation requires first-order input-output dynamics and smoothing of the high-frequency switching control (chattering effect) is of price of loosing robustness[31].

Due to the possibility of direct application of higher-order dynamics via the relative degree concept, the recently proposed Quasi-Continuous High-Order Sliding Modes (QCHOSM)[31,32] provide a convenient control approach to constructing robust controllers for uncertain higher-order systems such as aerospace systems[33-38]. The most outstanding feature of QCHOSM resides in the fact of the arbitrary increasing of the controller's order for the sake of enhanced performance and robustness without increasing the order of the system's dynamics. With QCHOSM, continuous control functions can be achieved without robustness degradation. To the author knowledge, the HOSM-based pole-placement is more recently investigated and relatively less researched[39,40].

The idea presented in this paper is to design a new Arbitrary-order Sliding Modes AOSM-based pole-placement scheme for Multi-Input-Multi-Output (MIMO) uncertain systems with arbitrary number and placement of poles for enhanced performance and robustness. The design is achieved through the pole-placement in QCHOSM gains adjustment. It is worth noting that the adjustment of QCHOSM controllers is recently investigated using different gain functions[41,42].

The target application of the proposed technique is the tactical missile autopilot design. Due to the large uncertainties of aerodynamic coefficients, missile dynamics are highly MIMO uncertain dynamics. A Two-channel pitch/yaw autopilot is designed to achieve enhanced finite-time stabilisation and control of a tail-controlled missile.

The remaining parts of the paper are organised as follows. In Section 2, the problem of multivariable QCHOSM is formulated. Section 3 describes the proposed AOSM-based pole-placement scheme. The dynamics of two-channel pitch/yaw missile are presented in Section 4 and application of AOSM-based pole-placement scheme to these dynamics is illustrated in Section 5. Conclusions and future works are given in Section 6.

https://doi.org/10.1017/S0001924000010812 Published online by Cambridge University Press

2.0 MULTIVARIABLE HOSM FORMULATION

The control objective in this study is to achieve a robust finite-time stability of a certain class of dynamical systems where the states are restrained to their zero-level in despite of internal and external disturbances. To do so, consider the following class of n-dimensional linear uncertain systems driven by an affine control input

$$\begin{cases} \dot{\boldsymbol{x}} = \mathbf{A}\boldsymbol{x} + \mathbf{B}\boldsymbol{u} + \boldsymbol{p} \\ \boldsymbol{y} = \mathbf{H}\boldsymbol{x} + \mathbf{D}\boldsymbol{u} \end{cases} \quad \ldots (1)$$

where $\boldsymbol{x} \in \mathbb{R}^n$, $\boldsymbol{u} \in \mathbb{R}^m$ and $\boldsymbol{y} \in \mathbb{R}^p$ are the system state, control input and output vectors, respectively. $\mathbf{A} \in \mathbb{R}^{n\times n}$ and $\mathbf{B} = :col\{\mathbf{b}_1, \mathbf{b}_2, \ldots, \mathbf{b}_m\} \in \mathbb{R}^{n\times m}$ are uncertain smooth functions. The vector $\mathbf{p}$ summarises all the internal disturbances, external disturbances and bounded measurement noises. The uncertainties of the matrices $\mathbf{A}$ and $\mathbf{B}$ are due to matched and unmatched disturbances.

The following basic concepts and assumptions are necessary for the establishment of higher-order sliding modes for multivariable uncertain systems (some of these propositions and assumptions are obtained by extending the propositions and assumptions stated in Ref. 31 for Single-Input-Single-Output SISO systems to MIMO systems).

Assumption A1: The uncertainties of system (1) are bounded

$$\begin{cases} \|\Delta\mathbf{A}\| \le \mathrm{a}_{\max} \\ \|\Delta\mathbf{B}\| \le \mathrm{b}_{\max} \end{cases} \quad \ldots (2)$$

where $a_{max} \in \mathbb{R}^+$ and $b_{max} \in \mathbb{R}^+$ are some positive constants.

Assumption A2: $\mathbf{H} = :row\{\mathbf{h}_1, \mathbf{h}_2, \ldots, \mathbf{h}_p\} \in \mathbb{R}^{n\times p}$ and $D = diag\{d_1, d_2, \ldots, d_p\}$.

Assumption A3: The unknown disturbance $\mathbf{p}$ is bounded with $||\mathbf{p}|| \le p_{max} \in \mathbb{R}^+$.

Assumption A4: The characteristic equation associated to the matrix $\mathbf{A}$ is a Hurwitz polynomial. The stability margin of system (1) is defined as follows:

$$\lambda_0 := \min_k\{-Re(\lambda_k)\} \quad \ldots (3)$$

where λ_k ($k = 1,\ldots,n$) are the eigenvalues of $\mathbf{A}$.

Corollary C1: System (1) is minimum-phase.

Corollary C2: The transfer functions $G_i^j(s) = \mathbf{h}_j(s\mathbf{I} - \mathbf{A})^{-1}\mathbf{b}_i + d_i$ are Bounded-Input-Bounded-Output (BIBO) stable.

Assumption A5: Each pair ($\mathbf{A}$, $\mathbf{b}_i$) is controllable and each pair ($\mathbf{A}$, $\mathbf{h}_j$) is observable. The controllability and observability matrices $\mathbf{C}_{\mu i}$ and $\mathbf{O}_{vj}$, respectively, are given by:

$$\begin{cases} \mathbf{C}_{\mu_i} = \left[\mathbf{b}_i \quad \mathbf{A}\mathbf{b}_i \quad \mathbf{A}^2\mathbf{b}_i \quad \ldots \quad \mathbf{A}^{\mu_i-1}\mathbf{b}_i\right] \\ \mathbf{O}_{v_j} = \left[\mathbf{h}_j^{\mathrm{T}} \quad (\mathbf{A}^{\mathrm{T}})\mathbf{h}_j^{\mathrm{T}} \quad (\mathbf{A}^{\mathrm{T}})^2\mathbf{h}_j^{\mathrm{T}} \quad \ldots \quad (\mathbf{A}^{\mathrm{T}})^{v_j-1}\mathbf{h}_j^{\mathrm{T}}\right] \end{cases} \quad i = 1,\ldots,m; j = 1,\ldots,p \quad \ldots (4)$$

μ_i and v_j are known constants.

Assumption A6: System (1) has a well-known and constant relative degree vector $\mathbf{r} = (r_1 \; r_2 \ldots r_p)^T$ where r_j ($j = 1,..,p$) are the local relative degree associated to the output y_j. According to Ref. 43, this assumption holds if and only if, the following properties hold for each output $y_j(\boldsymbol{x})$

https://doi.org/10.1017/S0001924000010812 Published online by Cambridge University Press

$$\forall \boldsymbol{x} \epsilon \mathbb{O}(\boldsymbol{x}_0): \begin{cases} \mathrm{L}_{\mathbf{f}}^{k} y_j(\boldsymbol{x}) = 0, & k = 0, \ldots, \mathrm{r}_j - 2 \\ L_{\mathbf{g}} \mathrm{L}_{\mathbf{f}}^{\mathrm{r}_i - 1} y_j(\boldsymbol{x}_0) \neq 0, \end{cases} \quad \ldots (5)$$

where $\mathbb{O}(\boldsymbol{x}_0)$ is an open neighbourhood of a given initial condition $\boldsymbol{x}_0$. $\mathrm{L}_f^{(k)}$) (.) and $L_g\, L_f^{r_j-1}$ (.) are the Lie derivatives.

Corollary C3: $\forall k = 0,1,\ldots, r_j - 2$, the conditions $\mathbf{h}_j\mathbf{A}^k\mathbf{b}_i = 0$ and $\mathbf{h}_j\mathbf{A}^{r_i-1}\mathbf{b}_i \neq 0$ hold.

Assumption A7: Since the control objective is to fulfill the condition $\boldsymbol{x} = 0$, each output y_j is associated with a sliding variable σ_j such that:

$$\sigma_j = \mathbf{c}_j^T \boldsymbol{x} \quad \ldots (6)$$

where $\boldsymbol{c}_j$ is a constant vector.

Assumption A8: System (1) is closed by discontinuous feedbacks u_i ($i = 1,\ldots,m$) and understood in Filippov's sense.

Assumption A9: If the sliding variables σ_j and their time derivatives up to $r_j - 1$ are continuous functions of $\boldsymbol{x}$, each set $\Gamma_j = \{\boldsymbol{x} | \sigma_j = \sigma_j^{(1)} = \ldots = \sigma_j^{(r_j-1)} = 0\}$ is a non-empty integral set of Filippov trajectories.

Corollary 4: Consider the case m = p, the motion on each set in assumption A9 is a ri-sliding mode with feedback control $u_i = U_i\,(\sigma_i, \sigma_i^{(1)},\ldots,\sigma_i^{(r_i-1)})$ where U_i is a bounded function.

Lemma 1 (31): The controllers u_i ($i = 1,..,m$) *are quasi-continuous controllers given by the following recursive formula*:

$$u_i = \mathrm{U}_i\left(\sigma_i, \sigma_i^{(1)}, \ldots, \sigma_i^{(r_i-1)}\right) = \alpha_i \Psi_{i,r_i-1}\left(\sigma_i, \sigma_i^{(1)}, \ldots, \sigma_i^{(r_i-1)}\right) \quad \ldots (7)$$

with;

$$\begin{cases} \Psi_{i,k}\left(\sigma_i, \sigma_i^{(1)}, \ldots, \sigma_i^{(r_i-1)}\right) = \varphi_{i,k}/N_{i,k} \\ for\ k = 0: \quad \Psi_{i,0} = \varphi_{i,0}/N_{i,0} = \sigma_i/|\sigma_i| \\ for\ k = 1, \ldots, r_i - 1: \ \Psi_{i,k} = \varphi_{i,k}/N_{i,k} \\ \varphi_{i,k} = \sigma_i^{(k)} + \beta_{i,k} N_{i,k-1}^{(r-k)/(r-k+1)} \Psi_{i,k-1} \\ N_{i,k} = \left|\sigma_i^{(k)}\right| + \beta_{i,k} N_{i,k-1}^{(r-k)/(r-k+1)} \end{cases} \quad \ldots (8)$$

where α_i ($i = 1,..,m$) are the controllers gains and $\beta_{i,k}$ are the controllers design parameters.

3.0 POLE PLACEMENT IN ARBITRARY-ORDER SLIDING MODES DESIGN

The control objective is to achieve a pole-placement in QCHOSM gains adjustment. The proper gains α_i in the control laws (Equation (7)) are obtained using higher orders of Ackermann-Utkin's formula through state functions. In this control problem, the states x_i are steered to their zero-level in despite of the disturbances p_i.

https://doi.org/10.1017/S0001924000010812 Published online by Cambridge University Press

3.1 Multivariable sliding modes using conventional Ackermann-Utkin technique

If $p = m$ in Equation (1) and if the input-output dynamics ($u_i \rightarrow \sigma_i$) are first-order dynamics, the multivariable system Equation (1) can be represented by a set of m subsystems controllable each by one control input u_i and a new decoupled auxiliary system is obtained:

$$\boldsymbol{\sigma}^r = \mathbf{L} + \mathbf{P}\boldsymbol{u} \quad \ldots (9)$$

where

$$\boldsymbol{\sigma}^r = \left[\sigma_1^{(r_1)}, \sigma_2^{(r_2)}, \ldots, \sigma_m^{(r_m)}\right]^T \quad \ldots (10)$$

$$\mathbf{L} = \left[\mathrm{L}_\mathbf{f}^{r_1}\sigma_1, \mathrm{L}_\mathbf{f}^{r_2}\sigma_2, \ldots, \mathrm{L}_\mathbf{f}^{r_m}\sigma_m\right]^T \quad \ldots (11)$$

$$\mathbf{P} = \begin{bmatrix} \mathrm{L}_\mathbf{g}\mathrm{L}_\mathbf{f}^{r_1-1} & 0 & \cdots & 0 \\ 0 & \mathrm{L}_\mathbf{g}\mathrm{L}_\mathbf{f}^{r_2-1} & \vdots & \vdots \\ \vdots & \vdots & \ddots & \vdots \\ 0 & 0 & \cdots & \mathrm{L}_\mathbf{g}\mathrm{L}_\mathbf{f}^{r_m-1} \end{bmatrix} \quad \ldots (12)$$

Applying the conventional Ackermann-Utkin sliding mode control law[24], the control input in system Equation (9) is given by:

$$\boldsymbol{u} = -row(\mathbf{K}\boldsymbol{x}) - [\omega_1\|\boldsymbol{x}\|sign(\sigma_1)\ \ \omega_2\|\boldsymbol{x}\|sign(\sigma_2)\ \ \cdots\ \omega_m\|\boldsymbol{x}\|sign(\sigma_m)\ ]^T \quad \ldots (13)$$

The matrix $\mathbf{K}$ can be constructed using Ackermann-Utkin formula:

$$\mathbf{K} = [0, 0, \ldots, 1][\mathbf{b}_i \quad \boldsymbol{A}\mathbf{b}_i \quad \boldsymbol{A}^2\mathbf{b}_i \quad \ldots \quad \boldsymbol{A}^{\mu_i-1}\mathbf{b}_i]^{-1}\vartheta(\boldsymbol{A}) \quad \ldots (14)$$

with:

$$\vartheta(\mathbf{A}) = \mathbf{A}^n + \sum_{k=1}^{n-1}\mu_k\mathbf{A}^{n-k} \quad \ldots (15)$$

where ω_i are some finite positive numbers and μ_k are the coefficients of the desired characteristic polynomial.

3.2 High-order sliding mode-based pole placement

According to Ref. 43, it is possible to extend the formula Equation (13) to systems of relative degrees higher than one. The extension of this statement to the case of MIMO systems is given as follows:

$$\boldsymbol{u} = -row\left(\frac{\mathbf{c}_i\mathbf{A}^{r_i}\boldsymbol{x} + \mathbf{z}(\mathrm{S}_i)}{\mathbf{c}_i\mathbf{A}^{r_i-1}\mathbf{b}_i}\right) \quad \ldots (16)$$

where the functions $z_i(S_i)$ are continuous functions of the sliding variables σ_i and their successive time derivatives $\sigma_i^{(k)}$ up to $r_i - 1$ (S_i are the coordinate sets of the variables $\sigma_i, \dot{\sigma}_i, .., \sigma_i^{(k)}$). In Ref. 38, the functions $z_i(S_i)$ were selected to be the following nested control functions:

https://doi.org/10.1017/S0001924000010812 Published online by Cambridge University Press

$$\begin{cases} z_i(\mathrm{S}_i) = \left(\sigma_i, \sigma_i^{(1)}, \ldots, \sigma_i^{(r_i-1)}\right) = \alpha_i\, \varphi_{i,k}/N_{i,k} \\ \varphi_{i,k} = sign\left(\sigma_i^{(k)}\right) + \beta_{i,k} N_{i,k} \varphi_{i,k-1} \\ N_{i,k} = \left(|\sigma_i\ |^{q/r} + \left|\sigma_i^{(1)}\right|^{q/(r-1)} + \cdots + \left|\sigma_i^{(k-1)}\right|^{q/(r-k+1)}\right)^{(r-k)/q} \end{cases} \quad \ldots (17)$$

and the matrices $\boldsymbol{c}_i$ in Equation (16) were constructed using the following zero-placement formula:

$$\mathbf{c}_i = [0, 0, \ldots, 1][\mathbf{b}_i \quad \mathbf{A}\mathbf{b}_i \quad \mathbf{A}^2\mathbf{b}_i \quad \ldots \quad \mathbf{A}^{\mu_i-1}\mathbf{b}_i]^{-1}\gamma_i(\lambda) \quad \ldots (18)$$

with:

$$\gamma_i(\lambda) = \lambda_i^{n-r_i} + \gamma_{i,n-r_i-1}\lambda_i^{n-r_i-1} + \cdots + \gamma_{i,1}\lambda_i + \gamma_{i,0} \quad \ldots (19)$$

The coefficients $\gamma_{i,k}$ are the coefficients of the numerators of the transfer functions:

$$G_i(s) = \mathbf{c}_i(s\mathbf{I} - \mathbf{A})^{-1}\mathbf{b}_i = \frac{s^{n-r_i} + \gamma_{i,n-r_i-1}s^{n-r_i-1} + \cdots + \gamma_{i,1}s + \gamma_{i,0}}{s^n + a_{i,n-1}s^{n-1} + \cdots + a_{i,1}s + a_{i,0}} \quad \ldots (20)$$

3.3 Arbitrary-order sliding modes-based pole-placement

Using the QHOSM control functions $\Psi_{i,ri-1}$ defined in Lemma 1, the controllers described in the following theorem are proposed as an enhanced alternative to the ones given by the control laws Equations (13) and (16).

Theorem 1: Consider that the assumptions A1-A9 hold, each controller

$$u_i = -\frac{\boldsymbol{c}_i\mathbf{A}^{r_i}\boldsymbol{\alpha}_i(\boldsymbol{x})}{\boldsymbol{c}_i\mathbf{A}^{r-1}\mathbf{b}_i}\Psi_i(\mathrm{S}_i) = -K_i\frac{\boldsymbol{c}_i\mathbf{A}^{r_i}\boldsymbol{x}}{\boldsymbol{c}_i\mathbf{A}^{r-1}\mathbf{b}_i}\Psi_{i,r_i-1}\left(\sigma_i, \sigma_i^{(1)}, \ldots, \sigma_i^{(r_i-1)}\right) \quad \ldots (21)$$

ensures the appearance of the r_i sliding mode $\sigma_i \equiv 0$ attracting trajectories in finite-time provided that the gains K_i in Equation (21) and the parameters $\beta_{i,k}$ in the recursive Equation (8) be properly chosen.

The desired dynamics are introduced through the zeros of the transfer functions in Equation (20). To compute the successive time-derivatives $\sigma_i^{(k)}$ needed in Equation (21), the following numerical scheme is considered:

$$\begin{cases} k = 1: & \sigma_i^{(1)} = \frac{s}{\tau s+1}\sigma_i \\ k = 2 & \sigma_i^{(2)} = \left(\frac{s}{\tau s+1}\right)^2\sigma_i \\ & \vdots \\ k = r-1 & \sigma_i^{(r-1)} = \left(\frac{s}{\tau s+1}\right)^{r-1}\sigma_i \end{cases} \quad \ldots (22)$$

where τ_i are the filters time constants.

4.0 MISSILE DYNAMICS

Bank-to-turn (BTT) control is one of the two modes commonly used in the missile guidance and control systems. In BTT mode, the roll rate is much larger than the pitch and yaw rates and the

https://doi.org/10.1017/S0001924000010812 Published online by Cambridge University Press

roll dynamics can be decoupled from pitch-yaw ones such that two autopilots can be designed: roll channel autopilot and pitch-yaw channel autopilot. Even the roll autopilot design is easy, the guidance and control of BTT missile along pitch-yaw channel is a challenging problem. In this Section, a time-varying linear pitch-way model is considered[44]

$$\begin{cases} \dot{\boldsymbol{x}} = \mathbf{A}\boldsymbol{x} + \mathbf{B}\boldsymbol{u} \\ \boldsymbol{y} = \mathbf{C}\boldsymbol{x} + \mathbf{D}\boldsymbol{u} \end{cases} \quad \ldots (23)$$

with:

$$\mathbf{A}(t) = \begin{bmatrix} \frac{\left(\frac{m_{mq}}{2V}L + m_z^{\dot{\alpha}}\right)qSL}{J_z} & \frac{m_z^{\alpha}}{J_z}qSL & \frac{J_x - J_y}{J_z}\omega_x & \frac{\left(m_z^{\beta} - m_z^{\dot{\alpha}}\omega_x\right)}{J_z}qSL \\ 1 & -\frac{c_y^{\alpha}}{Vm}qS & 0 & -\omega_x - \frac{c_y^{\beta}}{mV}qS \\ \frac{J_z - J_x}{J_y}\omega_x & \frac{\left(m_y^{\alpha} + m_y^{\beta}\omega_x\right)}{J_y}qSL & \frac{\left(\frac{m_{nr}}{2V}L + m_y^{\dot{\beta}}\right)}{J_y}qSL & \frac{m_y^{\beta}}{J_y}qSL \\ 0 & \omega_x + \frac{c_z^{\alpha}}{mV}qS & 1 & \frac{c_z^{\beta}}{mV}qS \end{bmatrix} \quad \ldots (24)$$

$$\mathbf{B}(t) = \begin{bmatrix} 0 & -\frac{c_z^{\alpha}qS}{mg} & 0 & \frac{\left(-c_x + c_z^{\beta}\right)qS}{mg} \\ 0 & \frac{(c_x + c_y^{\alpha})qS}{mg} & 0 & \frac{c_y^{\beta}qS}{mg} \end{bmatrix}^T \quad \ldots (25)$$

$$\mathbf{C}(t) = \begin{bmatrix} 0 & \frac{c_z^{\alpha}}{mg}qS & 0 & \frac{\left(-c_x + c_z^{\beta}\right)}{mg}qS \\ 0 & \frac{(c_x + c_y^{\alpha})}{mg}qS & 0 & \frac{c_y^{\beta}}{mg}qS \end{bmatrix} \quad \ldots (26)$$

$$\mathbf{D}(t) = \begin{bmatrix} \frac{c_z^{\delta_z}qS}{mg} & \frac{c_z^{\delta_y}qS}{mg} \\ \frac{c_y^{\delta_z}qS}{mg} & \frac{c_y^{\delta_y}qS}{mg} \end{bmatrix} \quad \ldots (27)$$

where $\boldsymbol{x} = (x_1\ x_2\ x_3\ x_4)^T = (\omega_z\ \alpha\ \omega_y\ \beta)^T \in \mathbb{R}^4$ is the system state vector, $\mathbf{A} \in \mathbb{R}^{4\times4}$ is a nonsingular matrix, $\mathbf{u} = (\delta_z\ \delta_y)^T \in \mathbb{R}^2$ is the control input vector to the missile system and $\mathbf{y} = (\eta_z\ \eta_y)^T \in \mathbb{R}^2$ is the missile commanded output vector. α and β are the angle-of-attack and sideslip angle; ω_z and ω_y are the pitch and yaw rates; η_z and η_y are the pitch and yaw overloads; δ_z and δ_y are the elevator and rudder deflections, respectively. The commanded control inputs $\delta_{z,c}$ and $\delta_{y,c}$ enter the system through the actuators dynamics that are described by the following second-order differential equation

$$\ddot{\delta} + 2\xi\omega_n\dot{\delta} + \omega_n^2\delta = \omega_n^2\delta_c \quad \ldots (28)$$

where δ and δ_c are, respectively, the actual and commanded tail-fin deflections of pitch channel or yaw channel. ω_n and ξ are the actuators natural frequency and actuators damping ratio, respectively.

https://doi.org/10.1017/S0001924000010812 Published online by Cambridge University Press

5.0 SIMULATION RESULTS AND ANALYSIS

In this Section, the results obtained through different simulation scenarios are discussed to evaluate the effectiveness, performance and robustness of the proposed AOSM-based pole-placement scheme. The first sample simulation scenario is considered for effectiveness demonstration and for comparison with a recently developed HOSM-based pole-placement scheme[38]. The second scenario is run using a Monte-Carlo stochastic simulation for robustness evaluation against modeling uncertainties. The third scenario is used to robustness validation in the presence of external disturbances in terms of measurement noises. The following form of the model (Equations (23)-(27) is considered for all the simulation scenarios:

$$\begin{cases} \dot{\boldsymbol{x}} = \begin{bmatrix} -1.8780 & -260.1298 & -5.2356 & 1.9895 \\ 1.0000 & -1.5060 & 0 & -6.9808 \\ 5.2356 & -2.0593 & -1.9500 & -39.7606 \\ 0 & 6.9808 & 1.0000 & -0.7710 \end{bmatrix} \boldsymbol{x} + \begin{bmatrix} -185.5729 & 0 \\ -0.2980 & 0 \\ 0 & -159.8991 \\ 0 & -0.2540 \end{bmatrix} \boldsymbol{u} \\ \boldsymbol{y} = \begin{bmatrix} 0 & 0 & 0 & -1.3716 \\ 0 & 2.6792 & 0 & 0 \end{bmatrix} \boldsymbol{x} + \begin{bmatrix} 0 & -0.4519 \\ 0.5301 & 0 \end{bmatrix} \boldsymbol{u} \end{cases} \quad \ldots (29)$$

The actuators characteristics are selected as follows:

$$\begin{cases} \omega_n = 150 \frac{rad}{s} \\ \xi = 0.7 \\ |\delta_{z,max}| \leq 45^{\circ}, |\delta_{y,max}| \leq 45^{\circ} \end{cases} \quad \ldots (30)$$

The controllability and observability of system Equation (29) is checked through the ranks of the controllability and observability matrices **U** and **V**:

$$\begin{cases} rank(\mathbf{U}) = rank([\mathbf{B} \quad \mathbf{AB} \quad \mathbf{A^2B} \quad \mathbf{A^3B}]) = 4 = dim(\boldsymbol{x}) \\ rank(\mathbf{V}) = rank([\mathbf{C}^{\mathrm{T}} \quad \mathbf{A}^{\mathrm{T}}\mathbf{C}^{\mathrm{T}} \quad (\mathbf{A}^{\mathrm{T}})^2\mathbf{C}^{\mathrm{T}} \quad (\mathbf{A}^{\mathrm{T}})^3\mathbf{C}^{\mathrm{T}}]) = 4 = dim(\boldsymbol{x}) \end{cases} \quad \ldots (31)$$

The open-loop characteristic polynomial is:

$$\gamma(\mathbf{A}) = \lambda^4 + 6{\cdot}1050\lambda^3 + 3{\cdot}8957e2\lambda^2 + 1{\cdot}0546e3\lambda + 1{\cdot}3622e3 \quad \ldots (32)$$

with the following roots:

$$\begin{cases} \lambda_{1,2} = -1{\cdot}6687 \pm 19{\cdot}337i \\ \lambda_{3,4} = -1{\cdot}3838 \pm 1{\cdot}3043i \end{cases} \quad \ldots (33)$$

5.1 Sample run for validation and comparison

In the present scenario, the proposed AOSM-based pole-placement scheme is validated for arbitrary numbers and locations of poles and the results are compared to those obtained by the HOSM-based pole-placement algorithm presented in Ref. 38. Using pitch control channel, different non-oscillatory stable poles are simulated starting from the following initial states

$$\boldsymbol{x}(0) = [\,75 \;\; 15 \;\; -150 \;\; -5]^T \quad \ldots (34)$$

https://doi.org/10.1017/S0001924000010812 Published online by Cambridge University Press

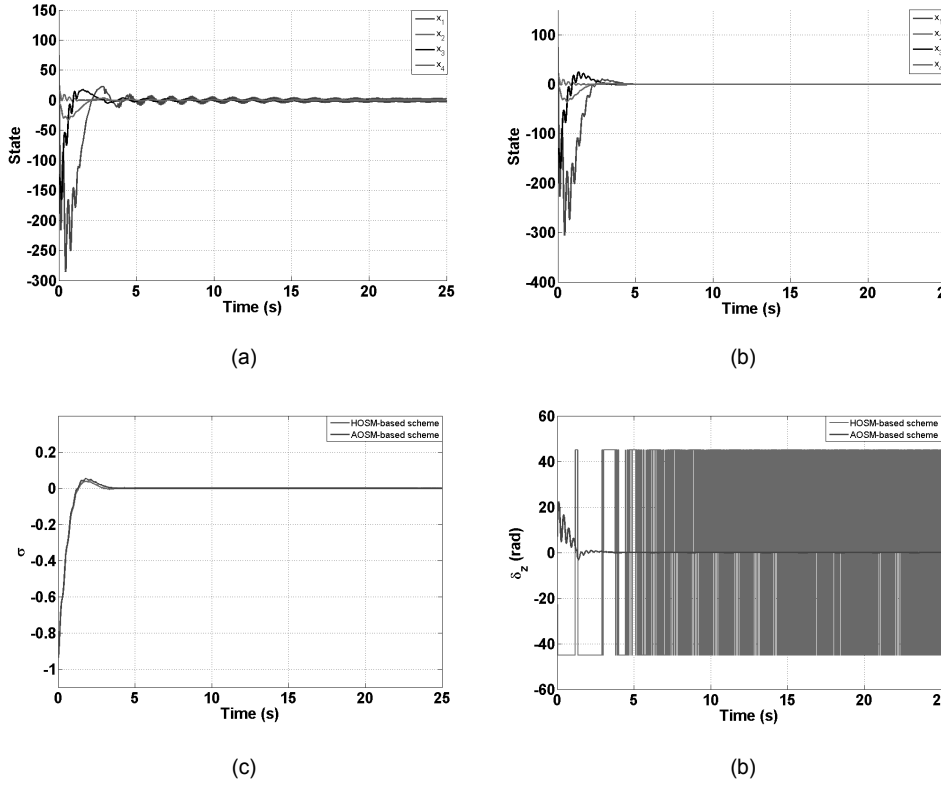


Figure 1 System responses to first-order sliding mode control: a) HOSM-based states, b) AOSM-based states, c) sliding variables, d) δ_z control efforts.

A. Placement of one pole

$$\gamma(\lambda) = (\lambda + 25) \quad \ldots (35)$$

$$c_1 = \begin{bmatrix} 4{\cdot}5222e-04 & -1{\cdot}3141e-03 & 6{\cdot}1866e-06 & -3{\cdot}8946e-03 \end{bmatrix} \quad \ldots (36)$$

B. Placement of two poles

$$\gamma(\lambda) = (\lambda + 10)^2 \quad \ldots (37)$$

$$c_1 = \begin{bmatrix} -1{\cdot}2399e-03 & 7{\cdot}3937e-02 & 4{\cdot}8645e-05 & -3{\cdot}0623e-02 \end{bmatrix} \quad \ldots (38)$$

C. Placement of three poles

$$\gamma(\lambda) = (\lambda + 20)(\lambda + 15)(\lambda + 3) \quad \ldots (39)$$

https://doi.org/10.1017/S0001924000010812 Published online by Cambridge University Press

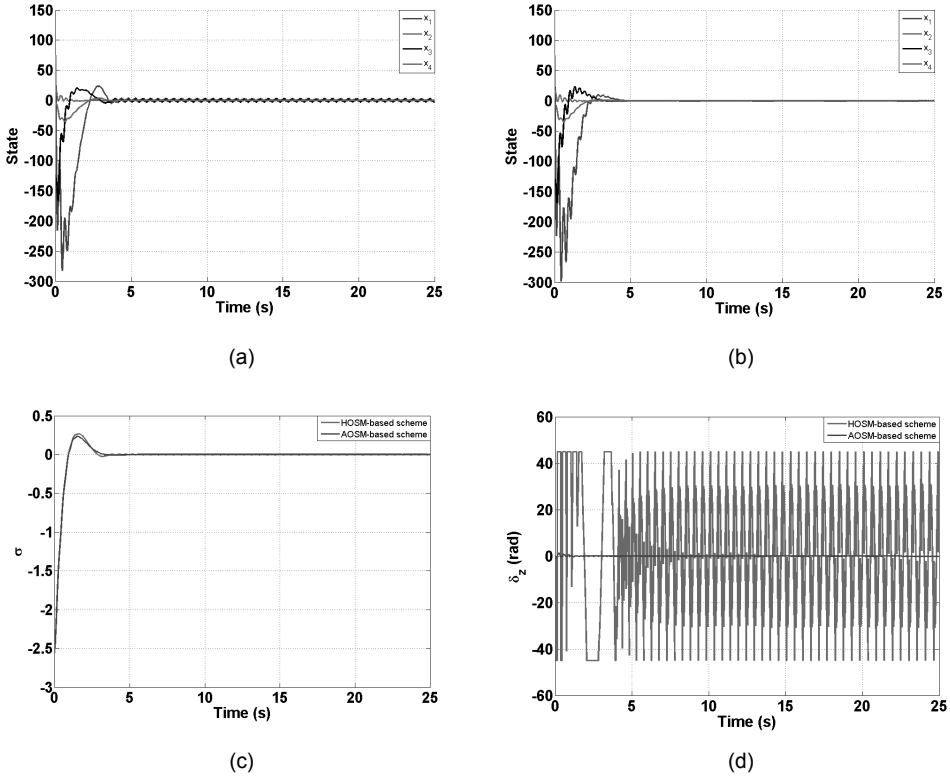


Figure 2. System responses to second-order sliding mode control:
a) HOSM-based states, b) AOSM-based states, c) sliding variables, d) δ_z control efforts.

$$\boldsymbol{c}_1 = [\,-4{\cdot}7085e-03 \quad -4{\cdot}2357e-01 \quad 4{\cdot}5995e-02 \quad -7{\cdot}1308e-02] \quad \ldots(40)$$

5.2 Monte-Carlo simulation

To evaluate the robustness of the AOSM-based pole-placement scheme against parameter uncertainties and modelling errors, a stochastic parameter uncertainty conditions are considered using a Monte-Carlo simulation of 500 sample runs. In this simulation, four poles are arbitrary located in the left side of the complex plane using the yaw control channel

$$\gamma(\lambda) = (\lambda+75)(\lambda+30)(\lambda+5)^2 \quad \ldots(41)$$

The missile parameters in all matrices of the model Equation (29) are varied randomly for 50% under-estimation to 50% over-estimation (i.e. ±50%). The resulting missile states, sliding variable σ and control input δ_y are shown, in terms of means, in Fig. 4.

5.3 Control in presence of measurement noises

The sensitivity of the controllers Equation (21) to the measurement noises is evaluated in the present simulation scenario. To produce noisy signals, zero-mean additive white Gaussian noises with standard deviation of 5 deg and 5 deg/s are added to the states α and β and ω_y and ω_z,

https://doi.org/10.1017/S0001924000010812 Published online by Cambridge University Press

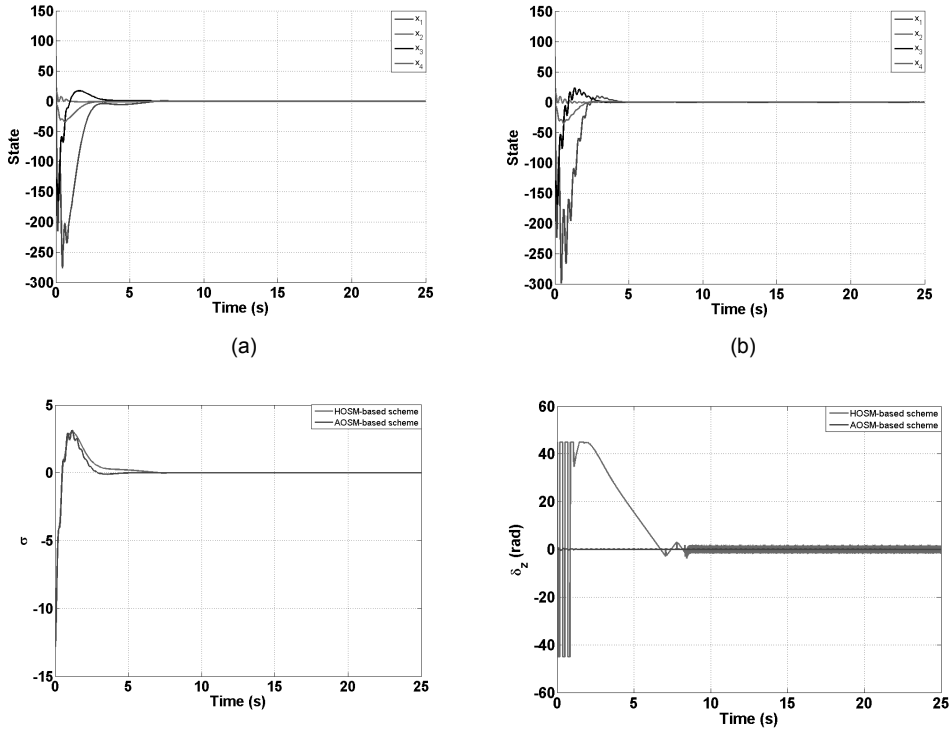


Figure 3. System responses to third-order sliding mode control: a) HOSM-based states, b) AOSM-based states, c) sliding variables, d) δ_z control efforts.

respectively. Figure 5 depicts the results of the placement of the following five poles in presence of measurement noises

$$\gamma(\lambda) = (\lambda + 125)(\lambda + 50)^2(\lambda + 3)^2 \quad \ldots (42)$$

In the first sample run validation, the nominal form of the model Equation (29) was used to perform arbitrary pole assignments (number and location). The four states of the system were driven to their zero-level with desired closed-loop poles (i.e. desired closed-loop performance). Figures 1-3 indicate the following outstanding characteristics of the proposed AOSM-based pole-placement scheme

- AOSM-based pole-placement scheme performs better than HOSM-based pole-placement.
- AOSM-based pole assignment improves the asymptotic tracking accuracy and the convergence rate.
- The arbitrary assignment of stable poles through AOSM-based pole placement scheme smoothens the control input and reduces its amplitude without degrading the system's performance.

In the second simulation scenario, uncertain forms of the model Equation (29) were used. The perturbed model forms were obtained using a stochastic Monte-Carlo method with 500 randomly selected perturbation terms and bounded parameter uncertainties of ±50%. The results of this

https://doi.org/10.1017/S0001924000010812 Published online by Cambridge University Press

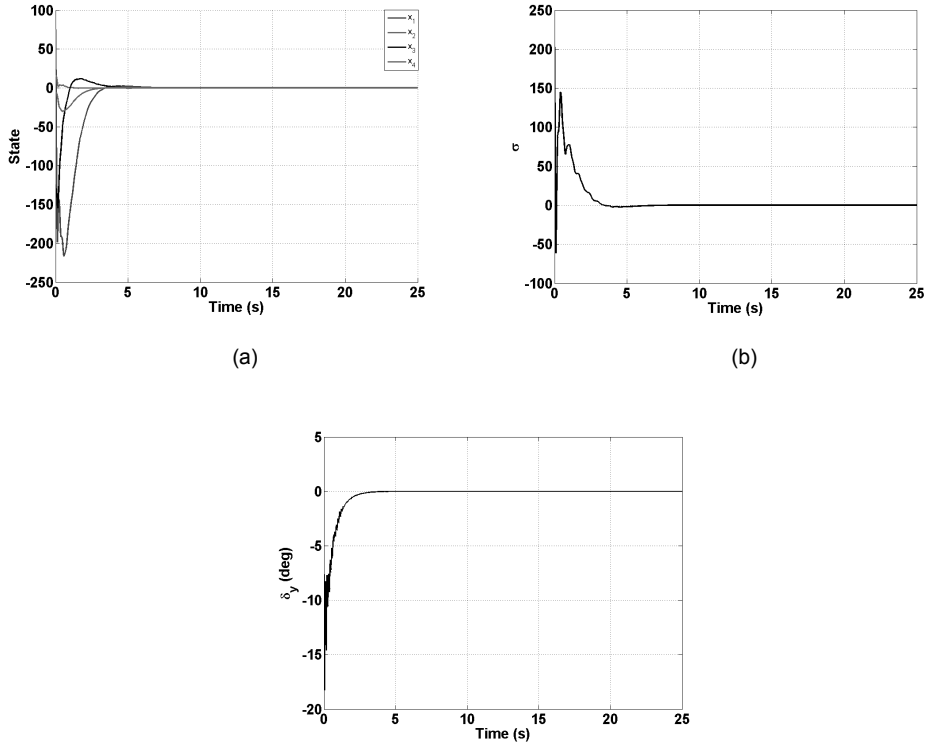


Figure 4. System responses to fourth-order sliding mode control with stochastic uncertainties: a) system states, b) sliding variable, c) δ_y control effort.

simulation scenario are depicted in Fig. 4. A comparison between AOMS-based pole placements using the nominal and perturbed closed-loop systems confirms the aforementioned advantages of the AOSM-based pole placement scheme even in the presence of heavy parameter uncertainties. The third simulation scenario was run in the presence of small measurement noises. The results illustrated in Fig. 5 show that the AOSM-based pole-placement feedback control is robust with respect to bounded zero-mean additive white Gaussian noises.

It is worth noting that even the states x_1 and x_3 exhibit non-harmful oscillations, all the states converge to their zero-level in a short period of time (5 seconds) in spite of parameter uncertainties and noises. By a proper selection of the control design parameters in the law Equation 21 using optimal tuning procedure, the oscillations of the states x_1 and x_3 can be damped and the performance of the whole system can be enhanced.

6.0 CONCLUSION

In this paper, we have shown that there are important advantages in using arbitrary-order sliding modes for pole-placement in dynamical systems. A pole-placement scheme based on artificial

https://doi.org/10.1017/S0001924000010812 Published online by Cambridge University Press

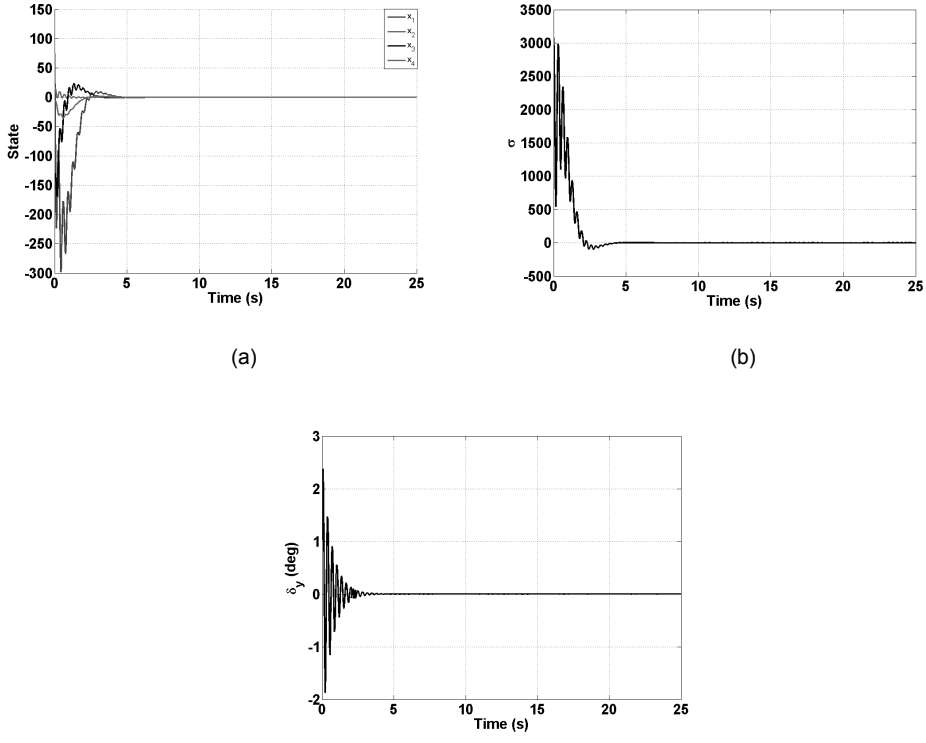


Figure 5. System responses to fifth-order sliding mode control with measurement noises: a) system states, b) sliding variable, c) δ_y control effort.

increase of poles number and arbitrary change in their location is presented. More enhanced performance, strong robustness and smooth control have been obtained as increasing the order of the controllers. The proposed scheme gave superior performance as compared against one of the recently published higher-order sliding modes-based pole-placement techniques.

There are many possible extensions as future work. An immediate one is to extend the application of the AOSM-base pole-placement scheme to the case of nonlinear systems using advanced linearisation techniques such as polytopic linear modeling and norm-bounded linear differential inclusions. Future work will also consider nonlinear systems operating under matched and unmatched uncertainties, unification and optimality of arbitrary pole assignments, non-minimum phase systems, stochastic systems and large dimension systems.

ACKNOWLEDGEMENTS

This article was funded by the Deanship of Scientific Research (DSR), King Abdulaziz University, Jeddah. The author, therefore, acknowledges with thanks DSR technical and financial support.

https://doi.org/10.1017/S0001924000010812 Published online by Cambridge University Press

REFERENCES

1. RAMI, M.A., FAIZ, S.E., BENZAOUIA, A. and TADEO, F. Robust exact pole placement via an LMI-based algorithm, *IEEE Transactions on Automatic Control*, 2009, **54**, pp 394–398.
2. JIAN, X. and FUZHONG W. For a class of uncertain linear systems robust reliable poles placement in disk regions, *Computing technology and automation*, 2010, **29**, (3), pp 1-5.
3. ATAEI, M. and ENSHAEE, A. Eigenvalue assignment by minimal state-feedback gain in LTI multivariable systems, *Int J Control*, 2011, **84**, pp 1956-1964.
4. HELMY, T. and ABDELAZIZ, S. Robust pole placement for second-order linear systems using velocity-plus-acceleration feedback, *IET Control Theory & Applications*, 2013, **7**, (14), pp 1843-1856.
5. LI, T. and CHU, E.K-W. Pole assignment for linear and quadratic systems with time-delay in control, *Numerical linear Algebra with Applications*, 2013, **20**, pp 291-301.
6. MAO, X. and DAI, H. Partial Eigenvalue assignment with time-delay robustness, *Numerical Algebra, Control and Optimization*, 2013, **3**, (2), pp 207-221.
7. SCHMID, R., PANDEY, A. and NGUYEN, T. Robust pole placement with Moore's algorithm, *IEEE Transactions on Automatic Control*, 2014, **59**, pp 500-505.
8. NTOGRAMATZIDIS, L. and SCHMID, R. Robust eigenstructure assignment in geometric control theory, *SIAM J on Control and Optimization*, 2014, **52**,(2), pp 960-986.
9. LE, X. and WANG, J. Robust pole assignment for synthesizing feedback control systems using recurrent neural networks, *IEEE Transactions on Neural Networks and Learning Systems*, 2014, **25**, (2), pp 383-393.
10. RAMI, M.A., FAIZ, S.E. and BENZAOUIA, A. Robust Exact Pole Placement via an LMI-Based Algorithm, *IEEE Transactions on Automatic Control*, 2009, **54**, (2), pp 394-398.
11. MISRIKHANOV, M.S. and RYABCHENKO, V.N. Pole placement in large dynamical systems with many inputs and outputs, *Doklady Mathematics*, 2011, **84**, (1), pp 591-593.
12. DATTA, S., CHAKRABORTY, D. and CHAUDHURI, B. Partial pole placement with controller optimization, *IEEE Transactions on Automatic Control*, 2012, **57**, (4), pp 1051-1056.
13. HELMY, T. and ABDELAZIZ, S. Robust pole placement for second-order linear systems using velocity-plus-acceleration feedback, *IET Control Theory Applications*, 2013, **7**, (14), pp 1843-1856.
14. ZUBOV, N.E., MIKRIN, E.A., MISRIKHANOV, M.S. and RYABCHENKO, V.N. Modification of the exact pole placement method and its application for the control of spacecraft motion, *J Computer and Systems Sciences International*, 2013, **52**, (2), pp 279-292.
15. ARUNA, B. and DEVANATHAN, R. Modified N-P interpolation theory for closed loop pole placement, *Asian J Control*, 2014, pp 1-9.
16. CHEKHOZADSKIKH, A.V. Extremal pole placement in control systems with a low order controller, *Automation and Remote Control*, 2014, **75**, (10), pp 1717-1731.
17. MILLER, D.E. and VALE, J.R. Pole placement adaptive control with persistent jumps in the plant parameters, *Mathematics of Control, Signals* and *Systems*, 2014, **26**, pp 177-214.
18. DATTA, S. and CHAKRABORTY, D. Feedback norm minimisation with regional pole placement, *International J Control*, 2014, **87**, (11), pp 2239-2251.
19. LE, X. and WANG, J. Robust Pole assignment for synthesizing feedback control systems using recurrent neural networks, *IEEE Transactions on Neural Networks and Learning Systems*, 2014, **25**, (2), pp 383-393.
20. PANDEY, A., SCHMID, S., NGUYEN, N., YANG, Y., SIMA, V. and TITS, A.L. performance survey of robust pole placement methods, IEEE Conference on Decision and Control, 2014, Los Angeles, California, USA.
21. PYRAGAS, V. and PYRAGAS, K. Continuous pole placement method for time-delayed feedback controlled systems, *The European Physical Journal B*, 2014, **87**, (274), pp 1-10.
22. SCHMID, R., PANDEY, A. and THANG, N. Robust pole placement with moore's algorithm, *IEEE Transactions On Automatic Control*, 2014, **59**, (2), pp 500-505.
23. SCHMID, R., NTOGRAMATZIDIS, L., NGUYEN, T. and PANDEY, A. A unified method for optimal arbitrary pole placement, *Automatica*, 2014, **50**, pp 2150-2154.
24. ACKERMANN, J. and UTKIN, V. Sliding mode control design based on Ackermann's formula, *IEEE Transactions on Automatic Control*, 1998, **43**, (2), pp 234-237.
25. MEZA, M.E.M. and BHAYA, A. Zero-placement approach to the design of sliding surfaces for linear multivariable systems, *IEE Proceedings - Control Theory and Applications*, 2001, **148**, (5), pp 333 - 339.
26. HA, P.O., TRINH, H. and NGUYEN, H.T. Dynamic output feedback sliding-mode control using pole placement and linear functional observers, *IEEE Transactions on Industrial Electronics*, 2003, **50**, (5), pp 1030-1037.
27. SINGLA, M., SHIEH, L.S., SONG, S., XIE, L. and ZHANG, Y. A new optimal sliding mode controller design using scalar sign function, *ISA Transactions*, 2014, **53**, pp 267-279.

https://doi.org/10.1017/S0001924000010812 Published online by Cambridge University Press

28. CRUZ-ZAVALA, E., MORENO, J.A. and FRIDMAN, L.M., Adaptive Gains Super-Twisting Algorithm for Systems with Growing Perturbations, Preprints of the 18th IFAC World Congress Milano (Italy), 28 August 2011 – 2 September 2011, pp 3039-3044.
29. KHANDEKAR, A.A., MALWATKAR, G.M. and PATRE, B.M. Discrete sliding mode control for robust tracking of higher order delay time systems with experimental application, *ISA Transactions*, **52**, 2013, pp 36-44.
30. PARKHI, P., BANDYOPDHYAY, B. and JHAA, M. Roll control using discrete-time robust sliding hyperplanes and fast output sampling, *J the Franklin Institute*, 2014, **351**, (4), pp 2107-2124.
31. LEVANT, A. Quasi-continuous high-order sliding-mode controllers, *IEEE Transactions on Automatic Control*, 2005, **50**, (11), pp 1812-1816.
32. LEVANT, A. and LIVNE, M. Uncertain disturbances attenuation by homogeneous multi-input multi-output sliding mode control and its discretisation, *IET Control Theory & Applications*, 2015, pp 1-11.
33. KADA, B. A novel higher-order sliding mode control scheme for uncertain nonlinear systems: short-period missile control application, *Int J Sciences: Basic and Applied Research (IJSBAR)*, 2015, **19**, (1), pp 398-409.
34. KADA, B. Arbitrary-order sliding-mode-based homing-missile guidance for intercepting highly maneuverable target, *J Guidance, Control* and *Dynamics*, 2014, **37**, (6), pp 1999-2013.
35. WANG, J., ZONG, Q., TIAN, B. and WANG, F. Flight control for hypersonic vehicle based on quasi-continuous integral high-order sliding mode, 24th Chinese Control and Decision Conference, 2012, pp 2185-2190.
36. ZANG, X. and TANG, S. Combined Feedback Linearization and Sliding Mode Control for Reusable Launch Vehicle Reentry, 2012, 12th International Conference on Control, Automation, *Robotics & Vision*, pp 1175-1180
37. PUKDEBOON, C., ZINOBER, A.S.I. and THEIN, M.W.L. Quasi-continuous higher order sliding-mode controllers for spacecraft-attitude-tracking manoeuvres, *IEEE Transactions on Industrial Electronics,* 2010, **05**, pp 215-220.
38. WANG, J., ZONG, Q., TIAN, B. and WANG, F. Flight control for a flexible air-breathing hypersonic vehicle based on quasi-continuous high-order sliding mode, *J Systems Engineering and Electronics*, **24**, (2), pp 288-295.
39. HERNÁNDEZ, D., CASTAÑOS, F. and FRIDMAN, L.M. Pole-placement in higher-order sliding-mode control, Preprints of the 19th IFAC World Congress, 24-29 August 2014, pp 1386-1391.
40. KHAN, Q. and BHATTI, A.I. Robust dynamic integral sliding mode for MIMO nonlinear systems operating under matched and unmatched uncertainties, *Control Engineering and Applied Informatics*, 2014, **16**, (4), pp 107-117.
41. LEVANT, A. and MICHAEL, A. Adjustment of high-order sliding-mode controllers, *International J Robust and Nonlinear Control*, 2009, **19**, pp 1657-1672.
42. ESTRADA, A. and FRIDMAN, L. Quasi-continuous HOSM control for systems with unmatched perturbations, *Automatica*, 2014, **46**, (11), pp 1916-1919.
43. BYRNES, C.I. and ISIDORI, A. Asymptotic stabilization of minimum phase nonlinear systems, *IEEE Transaction on Automatic Control*, 1991, **36**, pp 1122-1137.
44. TAN, F., HOU, M. and ZHAO, H. Autopilot design for homing missiles considering guidance loop dynamics, 2nd International Conference on Intelligent Control and Information Processing (ICICIP), 2011.

https://doi.org/10.1017/S0001924000010812 Published online by Cambridge University Press